Semiconductor Physics, Quantum Electronics & Optoelectronics, 2026. V. 29, No 1. P. 045-050.

Semiconductor physics

Comparing mean coordination dependences of elastic moduli and densities of stoichiometric and non-stoichiometric lines of Ge–As–S ternary glasses

V.M. Mitsa

Uzhhorod National University, 89A Zankovetskoi Street, 88015 Uzhhorod, Ukraine
E-mail: v.mitsa@gmail.com

Abstract. Binary As(Ge)–S and ternary Ge–As–S glasses along stoichiometric (quasi-binary) $As_{0.40}S_{0.60}$–$Ge_{0.33}S_{0.67}$ and non-stoichiometric $As_{0.35}S_{0.65}$–$Ge_{0.35}S_{0.65}$, $As_{0.40}S_{0.60}$–$Ge_{0.40}S_{0.60}$, and Ge–$As_{0.40}S_{0.60}$ lines were studied to understand the role of the mean coordination number (glass composition) on determining the physical properties of the glasses such as elastic moduli and density. A new information about the behavior of the physical parameters near the well-known "magic" mean coordination numbers at varying the glass composition was obtained. This is important from the practical point of view for topological nanoengineering and designing new glass compositions. A comparative analysis of elastic and density characteristics of sulfur- and germanium-rich lines with respect to those of quasi-binary As_2S_3–GeS_2 line was carried out. The structure of the glasses was considered in the framework of the concept of heterogeneous ordering during melt nanoclusterization by quenching. The structures of different types of crystal compounds known for binary As(Ge)–S systems were analyzed to identify correlations between the properties and structural characteristics (topology, stoichiometry, and dimensionality) of the glasses.

Keywords: binary As(Ge)–S and ternary Ge–As–S glasses, elastic modulus, density, mean coordination numbers, glass structure.

https://doi.org/10.15407/spqeo29.01.045
PACS 61.43.Fs, 62.20

Manuscript received 05.08.25; revised version received 12.02.26; accepted for publication 18.03.26; published online 25.03.26.

1. Introduction

Over recent decades, theoretical developments of physics of floppy-rigid transitions in glasses enabled making a big step toward understanding the regularities of glass formation [1–9]. The ease of glass formation [1, 2] was related to the ratio of the number of available degrees of freedom and the constraints number. It is known that constituent particles in floppy networks bind by rigid links. The total number of the constraints imposed by these links is smaller than that required for global rigidity of the system. This corresponds to the criterion of mechanical stability at a mean coordination number $z = 2.4$ [1, 2], at which the number of floppy modes is zero. The mentioned point corresponds to a strong tendency of making glass and was assigned to be a "rigidity transition" between a floppy network (unconstrained system) and a rigid one [1, 2]. It has been suggested later [10] that the floppy-to-rigid transition may not be abrupt at $z = 2.4$. According to the latter model, three elastic phases in glassy systems were identified: flexible ("floppy"), intermediate (IP) and stressed-rigid [10]. It is suggested in [10] that IP glasses would be completely resistant to aging or relaxation below melting temperature T_g [10]. It is common for the models presented in [1, 2, 10] that a rapid increase in the elastic moduli (C_{ij}) beyond z_{cr} (*e.g.* $C_{ij} = k(rp - 2.4)^{3/2}$) should be expected. Considering the presence of pyramidal and tetrahedral structural units in chalcogenide glassy matrices, a revised version of the topological constraint theory has recently been developed to describe the fraction of unconstrained degrees of freedom (f) [7]. This model predicts that glasses with $z = 2.4$ have underconstrained networks. Rapid increase in the elastic moduli is expected beyond $z = 2.67$ ($f = 0$) as the network becomes increasingly overconstrained [7]. Constraint-counting analysis for two-dimensional systems also predicts maximally stabilized composition at the same point. A structural phase transition from two- to three-dimensional networks is observed at $z = 2.67$ [11]. It is common for the models presented in [1–11] that a mean coordination number (z or f) directly or indirectly defines physical properties of chalcogenide glasses (ChG). Universal mean coordination dependences of physical properties of chalcogenide glasses are

attractive for topological nanoengineering [6] to search for new compositions for a number of practical applications [12–15]. Experimentally found compositions with critical values of the coordination number (z_c), predicted by most known theories, reveal that the values of z_c in binary glassy system are controversial [1, 2, 11]. In this regard, ternary system is an ideal testbed. For such systems, the value of z_c is expected to be a monotonic function of the average network connectivity.

In this work, we continue our study of rigidity of ChG glasses based on earlier studied As_ySi_{100-y} [16] and Ge_xS_{100-x} [17] binary systems. Moreover, a comparison with compositional (mean coordination number) dependences of longitudinal elastic moduli and density of a $Ge_xAs_ySi_{100-x}$ system along stoichiometric (quasi-binary) and non-stoichiometric lines is made.

2. Experimental details

Ultrasonic measurements were carried out applying echo-overlap method used in [18]. The measurement samples were ground and polished. The transmission mode was applied to determine the longitudinal waves velocity v_l. The longitudinal elastic modulus is defined as $C_l = \rho v^2$, where ρ is the density of the glassy material.

The densities of the samples used for investigations were determined using an Accu II 1340 Gas Displacement Pycnometry System. The measured values were compared with respective literature data for binary As(Ge)–S and chalcogenides in the ternary Ge–As–S system [18–21]. The mean coordination number z of the investigated glasses was calculated by the standard procedure.

3. Results and discussion

As was mentioned in [16], the elastic moduli of a binary As_ySi_{1-y} glass increase with the average coordination number $z = 3y + 2(1 - y)$ up to $z = 2.4$, exhibiting a maximum at the composition corresponding to stoichiometric As_2S_3. A part of the curve $C_l = C_l(z)$ can be approximated by four linear functions with different slopes at the intervals $2.1 < z < 2.2$ (i), $2.2 \le z < 2.35$ (ii), $2.35 \le z \le 2.4$ (iii) and $2.4 \le z \le 2.43$ (iv). It is known that in the first region ($2.1 < z < 2.2$), where the As concentration decreases from 20 to 8 at.%, As_ySi_{100-y} glass networks rapidly segregate [10]. The glasses from this region tend to form a large number of floppy clusters weakly connected to the host matrix [10]. Interpreting Raman spectra enables identifying correlations with structural characteristics related to topology, stoichiometry and dimensionality [10, 16, 18, 22]. The local structure of such sulfur-rich As–S glasses can be characterized primarily by presence of S_8 rings and As–S–S–As and S_n chains [10, 16, 18].

However, increasing the As content also induces formation of As–S–S–As and As–S–As links in the glass structure [10, 22, 23]. Further increase of the As content corresponding to the second interval ($2.2 \le z < 2.3$) enhances covalent character of the As–S bonds in the glassy matrix and formation of ring-like $As_6S_{6+6/2}$

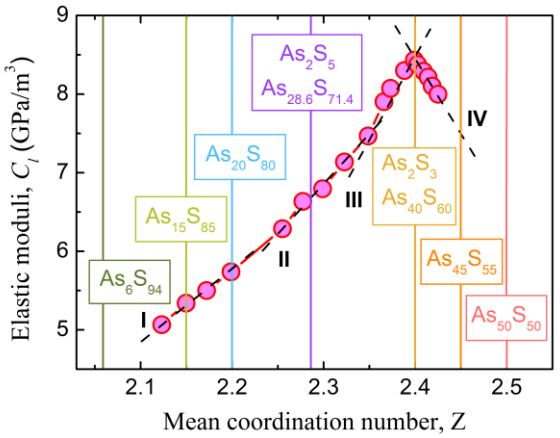

Fig. 1. Mean coordination number (z) dependence of longitudinal elastic moduli C_l in As_ySi_{100-y} binary system. The dashed lines are a guide for eyes which determines four linear regions [16].

nanoclusters [16, 23]. Consequently, the values of the elastic moduli of such glasses become higher, which corresponds to a more rigid structure. Such behavior is evidenced by the higher slope of the second linear function as compared to the first one. It was shown in [16, 22, 23] in the framework of the middle-range ordering approximation that the ring-like $As_6S_{6+6/2}$ nanoclusters, being primary building blocks of glassy (g) and crystalline (c) As_2S_3, may be responsible for the key features observed in the vibrational spectra of g-As_2S_3.

The highest slope is observed for the function in the third interval ($2.35 \le z \le 2.4$). Here, the composition approaches that of stoichiometric As_2S_3 with $z = 2.4$ (Fig. 1). The maximum values of C_l of As–S glasses at $z = 2.4$ demonstrate that stoichiometry mainly defines the physical properties [7, 10]. At this composition, chemical ordering in a pyramidal network is mainly caused by the ring-like $As_6S_{6+6/2}$ nanoclusters [18, 28]. Small inclusions of r-As_4S_4 realgar-like nanoclusters [23] are also present in the structure of g-As_2S_3 [10, 24]. The role of the ring-shaped clusters in formation of rigid structures was also considered for tetrahedral networks (a Ge–Se system) [30]. Formation and increasing number of weak metallic As–As bonds result in loss of connectivity. At this, the concentration of sulfur in As_xS_{100-x} glasses is reduced below the stoichiometric value ($x = 40$, $z = 2.4$). Indeed, enrichment of $As_{40}S_{60}$ with arsenic (*e.g.* $As_{42}S_{58}$, $z = 2.42$) leads to a decrease in the elastic moduli and deviation of their values from theoretical predictions [1, 2].

The fourth linear function ($2.4 \le z \le 2.43$) exhibits a negative slope due to decreasing C_l values at $z > 2.4$ (Fig. 1). Raman spectra of glassy $As_{45}S_{55}$ corresponding to the fourth interval ($z = 2.45$) show existence of inclusions of r-p-As_4S_4 nanoclusters of realgar and pararealgar structure [16, 23] as well as a small amount of As_4S_3 cage-like molecules with homopolar As–As bonds [25]. All the bonds of the mentioned structures are chemically saturated and, hence, only weak dispersive interaction of these molecules with the glass network based on ring-like $As_6S_{6+6/2}$ nanoclusters is possible [16].

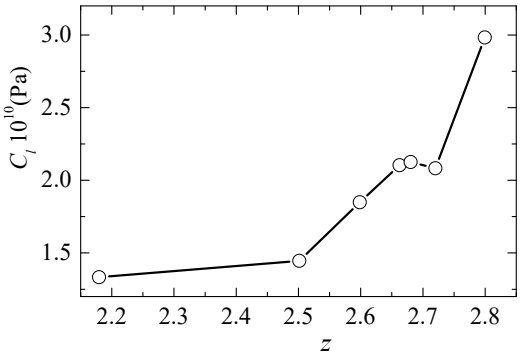

Fig. 2. Longitudinal elastic moduli C_l *versus* mean coordination number (z) for a Ge_xS_{100-x} binary system [17]. The lines are guide for eyes and determine three linear regions.

The longitudinal elastic moduli C_l in a Ge_xS_{100-x} binary system [17] monotonously increase with x ($z = 4x + 2(1 - x)/100$) up to $z = 2.8$. A flat part in the range of 2.67 (GeS_2) to 2.72 ($Ge_{36}S_{64}$) is observed in the dependence $C_l(z)$ (Fig. 2). Similarly to the As_yS_{100-y} glasses (Fig. 1), the curve $C_l = C_l(z)$ can be approximated by three linear functions with different slopes in the intervals $2.2 < z < 2.5$ (i), $2.5 \le z \le 2.67$ (ii), and $2.7 < z \le 2.8$ (iii) (Fig. 2). The first region ($2.2 < z < 2.5$) corresponds to sulfur-rich Ge–S glasses containing Ge–S–S–Ge and Ge–S–Ge links and S_8 rings [19]. It is known that S_8 rings that do not contribute to network formation [7]. Furthermore, clusters topologically similar to β-GeS_2, in which $GeS_{4/2}$ tetrahedrons form six- and four-member rings connected by a corner and an edge [26], begin to grow in the structure of sulfur-rich glasses. Increase of the Ge content above $x = 0.25$ ($z = 2.5$) increases the elastic moduli up to $z = 2.67$, see Fig. 2. The point $z = 2.67$ corresponds to stoichiometric g-GeS_2. We concluded before [26, 27] that from the structure point of view, a middle-range structural ordering is created in g-GeS_2 during melt clustering by quenching. At this, a mixture of corner-shared three-dimensional clusters, topologically similar to those in low-temperature α-GeS_2 crystals and two-dimensional high-temperature β-GeS_2 crystals, forms. In a layered β-GeS_2 crystalline structure, GeS_4 tetrahedral units are connected by edges or corners to produce six- and four-member rings in a 2:1 ratio. The similarity of the medium-range ordering of g-GeS_2 to that of α-GeS_2 was also confirmed by the study of α-GeS_2 microcrystals grown in g-GeS_2 during annealing at 497 °C, which is below the glass transition temperature [28]. According to the model [7], "one should expect a rapid increase in the elastic moduli beyond $z = 2.67$, since the network is increasingly overconstrained". Indeed, enrichment of glasses with Ge over the composition range $36 \le x \le 40$ ($2.72 \le z \le 2.8$) leads to an increase in the elastic moduli values achieving the maximum value for g-Ge_2S_3 ($Ge_{40}S_{60}$), see Fig. 2. Spectroscopic analyses showed that the contribution of corner-shared three-dimensional clusters, topologically similar to those in low-temperature α-GeS_2 crystals, is decreased in g-Ge_2S_3 as compared to g-GeS_2. Moreover, the relative amount of clusters typical for β-GeS_2, in which $GeS_{4/2}$ tetrahedra are connected by an edge, also decreases. The latter nanoclusters provide more degrees of freedom to the network as compared to their corner-sharing counterparts, since shared edges do not contribute to the connectivity of the rest of the network [7]. The extended X-ray absorption fine structure and anomalous wide-angle X-ray scattering (EXAFS and AWAXS) data [29] demonstrate that the degree of depolymerization of both corner-shared and edge-shared tetrahedra increases from 40% in g-GeS_2 to 70% in g-$Ge_{40}S_{60}$. A linear crystal growth kinetics of both α-GeS_2 and β-GeS_2 polymorphs has been also observed in g-$Ge_{42}S_{58}$ during heating over a relatively broad range of temperatures [28]. It was shown in our previous study [27] that the structure of glassy Ge_2S_3 (g-Ge_2S_3) consists of six-member $Ge_3S_{3+6/2}$ rings, four-member $Ge_2S_{2+4/2}$ rings, defective five-member $Ge_3S_{5+4/2}$ rings containing either S–S or Ge–Ge bonds, and clusters based on $Ge_{4/4}$ coordination units. The next main features of the Raman spectra of the glassy g-Ge_2S_3 may be interpreted as evidence of nanoclusters built from $SGe_{3/3}$ structural units that are topologically similar to those in crystalline GeS [27]. Such local coordination environments cannot be derived from calculations of the average mean coordination number z and constraint density f within the structural–topological transition model describing the increase in the glass rigidity, developed in [1, 2, 7, 10].

Then a certain amount of GeS_2 was added to As_2S_3 along the quasi-binary line As_2S_3–GeS_2 ($z = 2.42$, see curve *3* in Fig. 4 and Table), the clusters based on $GeS_{4/2}$ appeared and the values of the elastic moduli and C_l slightly increased at $z = 2.46$, 2.47. When the content of As_2S_3 and GeS_2 in the ternary glasses was approximately equal ($z = 2.5$, 2.52), phase separation of different-type structural units accompanied by slight decrease of C_l became possible [19] (see Fig. 4 and Table). At $z > 2.52$, the elastic moduli slightly increased at $z = 2.56$, 2.58 (Fig. 4 and Table). The structure of such glasses could be represented as a mixture of corner- and edge-sharing $GeS_{4/2}$ tetrahedra forming both six- and four-member rings interlinked with $AsS_{3/2}$ pyramids [31]. When composition (z) approached that of g-GeS_2 ($z = 2.6$), the value of C_l decreased (Fig. 4 and Table) and exhibited minimum at $z = 2.66$ (g-GeS_2). The structure of g-GeS_2 was considered above.

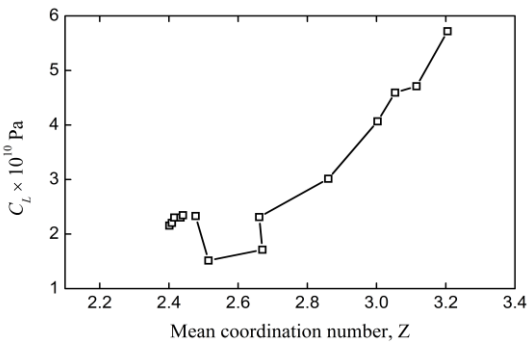

Fig. 3. Longitudinal elastic modules C_l of Ge–As_2S_3 ternary glasses *versus* mean coordination number (z). The lines are guide for eyes.

Table. Composition, longitudinal velocity, density and longitudinal elastic modulus along stoichiometric As_2S_3–GeS_2 line.

Composition, ar.%	z	V_l, 10^3 m/s	ρ, $\times 10^3$ kg/m^3	C_{11}, 10^{10} Pa
$As_{40}S_{60}$	2.4	2.57	3.19	2.11
$Ge_3As_{36}S_{61}$	2.42	2.61	3.17	2.16
$Ge_7As_{32}S_{61}$	2.46	2.62	3.15	2.16
$Ge_{10}As_{28}S_{62}$	2.48	2.64	3.06	2.13
$Ge_{13}As_{25}S_{62}$	2.5	2.65	3.03	2.13
$Ge_{17}As_{20}S_{63}$	2.52	2.67	3.0	2.14
$Ge_{20}As_{16}S_{64}$	2.56	2.71	2.98	2.18
$Ge_{23}As_{12}S_{65}$	2.58	2.73	2.92	2.17
$Ge_{26}As_8S_{66}$	2.6	2.74	2.82	2.12
$Ge_{33}S_{67}$	2.66	2.71	2.72	2.0

Adding a small amount of Ge to the stoichiometric As_2S_3 (Fig. 3, curve *5*) leads to generation of clusters based on $GeS_{4/2}$ s.u. (structural units) in ternary glasses, accompanied by slight increase of C_l with a small maximum near $z = 2.45$. Since Ge–S bonds in the $GeS_{4/2}$ s.u. are energetically more favorable than As–S bonds [19], increasing the Ge content in the $Ge_x(As_2S_3)_{100-x}$ glasses causes deficiency of sulfur. That is why further increase of the germanium (x) content ($z > 2.45$), similarly to the As–S glasses, is accompanied by formation of inclusions of As-rich r-p-As_4S_4 nanocrystals with realgar and pararealgar structure as well as a small amount of As_4S_3 cage-like molecules in the structure of the glasses [22–25]. This leads to disconnecting of the structural matrix of the ternary glass and decrease of C_l at $2.45 < z > 2.66$ (Fig. 4, curve *5*). A noticeable increase of the values of elastic moduli in the Ge–As_2S_3 glasses is clearly observed at $z > 2.67$. The major role in the formation of a rigid structure of such glasses during quenching is played by generated clusters based on six-member rings $Ge_3S_{3+6/2}$, defective five-member rings $Ge_3S_{5+4/2}$ (S–S) and $Ge_3S_{5+4/2}$ (Ge–Ge), and clusters based on $SGe_{3/3}$ s.u., topologically similar to those in c-GeS [27]. The value of C_l in the sulfur-deficient Ge–As_2S_3 glasses is the highest among all the studied compositional lines in the $C_l(z)$ dependence for Ge–As–S glasses (Fig. 4, curve *5*), except for a single point at $z = 2.6$ where the C_l value coincides with that of a glass from the quasi-binary As_2S_3–GeS_2 As line (Fig. 4, curve *3*).

Adding a small amount of Ge_2S_3 to As_2S_3 leads to a drastic change of C_l and a non-monotonous decrease of C_l up to $z = 2.62$ (Fig. 3, curve *4*). It seems that the series of As_2S_5–Ge_2S_3 glasses at $2.4 < z < 2.62$ have a micro-heterogeneous structure [32]. Like the Ge–As_2S_3 glasses (Fig. 4, curve *5*), inclusions of r-p-As_4S_4 nanocrystals with realgar and pararealgar structure as well as a small amount of As_4S_3 cage-like molecules form in their structure [32]. For such glasses, formation of coexisting nuclei with middle-range ordering based on $AsS_{3/2}$, $GeS_{4/2}$ and $As_2S_{4/2}$ s.u. in their structure is typical [32].

For $z > 2.62$, the structure of the glasses becomes more rigid formed mainly by clusters based on $SGe_{3/3}$ s.u. and clusters based on $GeS_{4/2}$ tetrahedra connected by corner. A detailed analysis of the Raman spectra of ternary glasses and the results of DFT calculations for different cluster types will be presented elsewhere.

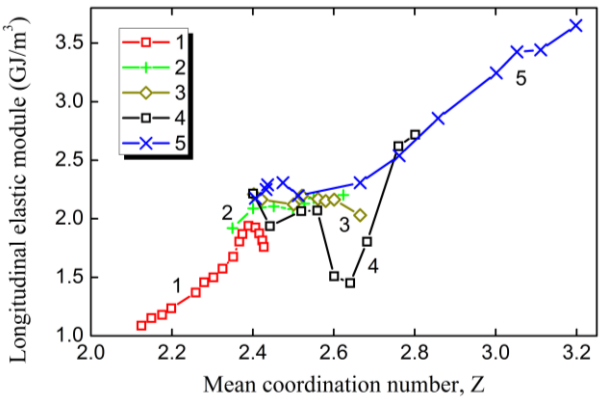

Fig. 4. Longitudinal elastic moduli of $Ge_xAs_yS_{1-x-y}$ glasses along the tin lines: *1* – As_yS_{1-y}, *2* – $As_{0.35}S_{0.65}$–$Ge_{0.35}S_{0.65}$, *3* – $As_{0.40}S_{0.60}$–$Ge_{0.33}S_{0.67}$, *4* – $As_{0.40}S_{0.60}$–$Ge_{0.40}S_{0.60}$, and *5* – Ge–$As_{0.40}S_{0.60}$ *versus* mean coordination number.

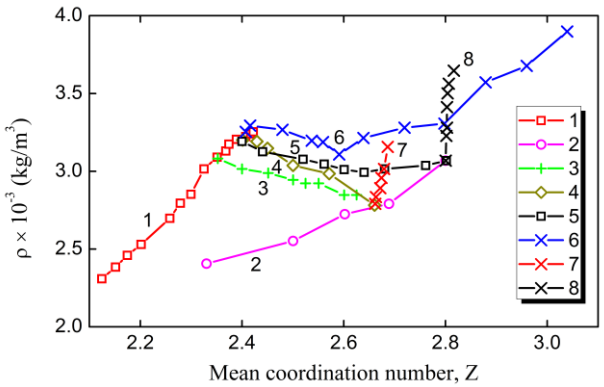

Fig. 5. Density of $Ge_xAs_yS_{1-x-y}$ glasses along the lines: *1* – As_yS_{1-y}, *2* – Ge_xS_{1-x} [19], *3* – $As_{0.35}S_{0.65}$–$Ge_{0.35}S_{0.65}$, *4* – $As_{0.40}S_{0.60}$–$Ge_{0.33}S_{0.67}$, *5* – $As_{0.40}S_{0.60}$–$Ge_{0.40}S_{0.60}$, *6* – Ge–$As_{0.40}S_{0.60}$, *7* – As–$Ge_{0.33}S_{0.67}$, and *8* – As–Ge_2S_3 *versus* mean coordination number.

According to [7], the glass softening temperature T_g in the Ge–As–Se system along different compositional lines exhibits a nearly universal dependence on f over a wide range of compositions. Such dependence is

attractive for topological universal engineering aimed at searching the compositions with rigid structure [6]. In our case, the Ge–As–S glass density dependence on z along different lines (Fig. 5) does not have universal character. Different compositions have different values of density at the same values of z. The unusual rapid growth of the density dependence on z for As–GeS_2 and As–Ge_2S_3 glasses (Fig. 5) demonstrates interpretation of the structure in the framework of the concepts composition (z) structure – properties may involve structural units formation in germanium-rich glasses, where Ge has triple coordination with sulfur.

4. Conclusions

- The experimental dependences of the longitudinal elastic modulus and density on the mean coordination number in ternary Ge–As–S glasses are inconsistent with the previously reported nearly universal dependence of the glass transition temperature (T_g) on the constraint f over a wide compositional range in Ge–As–Se systems. The latter relationship was considered in the framework of rigid polyhedra used to evaluate topological constraints. Variation of composition along different lines shows that the same average coordination number (z) does not correspond to identical values of density and C_l for each compositional line.
- For Ge–As–S glasses, sulfur-deficient Ge–As_2S_3 compositions exhibit the highest values of C_l and density over a broad compositional range ($2.4 < z < 3.22$) among all the studied compositional lines in the $C_l(z)$ dependence. The minimum C_l values in the range $2.4 < z < 2.66$ are observed for glasses along the $As_{0.40}S_{0.60}$–$Ge_{0.40}S_{0.60}$ compositional line.
- The rapid increase of C_l at $z > 2.67$, together with the anomalous density behavior of As–GeS_2 and As–Ge_2S_3 glasses, may be attributed to the formation of nanoclusters based on $SGe_{3/3}$ structural units that are topologically similar to those in crystalline GeS. Such local coordination environments was not accounted for in calculations based solely on the average coordination number z or the fraction of unconstrained degrees of freedom (f) within the revised structural–topological transition model.

References

1. Phillips J.C., Thorpe M.F. Constraint theory, vector percolation and glass formation. *Solid State Commun*. 1985. **53**. P. 699. https://doi.org/10.1016/0038-1098(85)90381-3.
2. He H., Thorpe M.F. Elastic properties of glasses. *Phys. Rev. Lett*. 1985. **54**. P. 2107. https://doi.org/10.1103/PhysRevLett.54.2107.
3. Gupta P.K. Rigidity, connectivity, and glass-forming ability. *J. Amer. Ceram. Soc*. 1993. **76**. P. 1088. https://doi.org/10.1111/j.1151-2916.1993.tb03725.x.
4. Bauchy M., Micoulaut M. Densified network glasses and liquids with thermodynamically reversible and structurally adaptive behaviour. *Nat. Commun*. 2015. **6**. P. 6398. https://doi.org/10.1038/ncomms7398.
5. Yildirim C., Raty J.-Y., Micoulaut M. Revealing the role of molecular rigidity on the fragility evolution of glass-forming liquids. *Nat. Commun*. 2016. **7**. P. 11086. https://doi.org/10.1038/ncomms11086.
6. Bauchy M. Nanoengineering of concrete *via* topological constraint theory. *MRS Bull*. 2016. **50**. P. 201742. https://doi.org/10.1557/mrs.2016.295.
7. Sen S., Mason J.K. Topological constraint theory for network glasses and glass-forming liquids: A rigid polytope approach. *Front Mater*. 2019. **6**. https://doi.org/10.3389/fmats.2019.00213.
8. Micoulaut M. Concepts and applications of rigidity in non-crystalline solids: A review on new developments and directions. *Adv. Phys. X*. 2016. **1**. P. 147–175. https://doi.org/10.1080/23746149.2016.1161498.
9. Yan L. Entropy favors heterogeneous structures of networks near the rigidity threshold. *Nat. Commun.* 2018. **9**. P. 1359. https://doi.org/10.1038/s41467-018-03859-9.
10. Chen P., Holbrook C., Boolchand P. *et al*. Intermediate phase, network demixing, boson and floppy modes, and compositional trends in glass transition temperatures of binary As_xS_{1-x} system. *Phys. Rev. B*. 2008. **78**. P. 224208. https://doi.org/10.1103/PhysRevB.78.224208.
11. Tanaka K. Structural phase transitions in chalcogenide glasses. *Phys. Rev*. 1989. **39**. P. 1270–1278. https://doi.org/10.1103/PhysRevB.39.1270.
12. Ding S., Dai S., Cao Z. *et al*. Composition dependence of the physical and acousto-optic properties of transparent Ge–As–S chalcogenide glasses. *Opt. Mater*. 2020. **108**. P. 110175. https://doi.org/10.1016/j.optmat.2020.110175.
13. Mitsa A.V., Mitsa V.M, Ugrin A.M. Mathematical modeling of spectral characteristics of optical coatings with slightly inhomogeneous chalcogenide films. *J. Optoelectron. Adv. Mater*. 2005. **7**. P. 955–962.
14. Pervak Y.A., Mitsa A., Holovach I., Fekeshgazi I.V. Influence of transition film-substrate layers on optical properties of the multilayer structures. *Proc. SPIE*. 2001. **4425**. P. 321–325.
15. Stronski A., Vlček M. Imaging properties of $As_{40}S_{40}Se_{20}$ layers. *Opto-electron. Rev*. 2000. **8**, No 3. P. 263–267.
16. Baloh P., Tkáč V., Tarasenko R. *et al*. The interplay between the topology of nanoclusters and the characteristic of boson peak in As-S glasses. *J. Non-Cryst. Solids.* 2024. **631**. P. 122913. https://doi.org/10.1016/j.jnoncrysol.2024.122913.
17. Babynets Yu.Yu. Vibrational spectra and structural correlations in $As_x(GeS_2)_{1-x}$ glasses and films based on them: *Abstract of the dissertation of the candidate of physical and mathematical sciences*: 01.04.07. Institute of Physics, NAS of Ukraine. Kyiv, 1995.
18. Tsiulyanu D., Kozyukhin S.A., Ciobanu M. Middle range order and elastic properties of non-stoichiometric chalcogenide glasses in the AsS_3-GeS_4 system. *J. Non-Cryst. Solids*. 2022. **575**. P. 121207. https://doi.org/10.1016/j.jnoncrysol.2021.121207.

19. Borisova Z.U. *Glassy Semiconductors*. Springer, 1981. https://doi.org/10.1007/978-1-4757-0851-6.
20. Stronski A., Kavetskyy T., Revutska L. *et al*. Structural order in $(As_2S_3)_x(GeS_2)_{1-x}$ glasses. *J. Non-Cryst. Solids*. 2021. **572**. P. 121075. https://doi.org/10.1016/j.jnoncrysol.2021.121075.
21. Andreichin R., Nikiforova M., Skordeva E. *et al*. Structure and physical properties of the glassy $As_2S_3Ge_x$ system. *J. Non-Cryst. Solids*. 1976. **20**. P. 101–122. https://doi.org/10.1016/0022-3093(76)90110-1.
22. Holomb R., Mitsa V., Johansson P., Veres M. Boson peak in low-frequency Raman spectra of As_xS_{100-x} glasses: Nanocluster contribution. *phys. status solidi (c)*. 2010. **7**, No 3–4. P. 885–888. https://doi.org/10.1002/pssc.200982829.
23. Holomb R., Kondrat O., Mitsa V. *et al*. Gold nanoparticle assisted synthesis and characterization of As–S crystallites: Scanning electron microscopy, X-ray diffraction, energy-dispersive X-ray and Raman spectroscopy combined with DFT calculations. *J. Alloys Compd.* 2022. **894**. P. 162467. https://doi.org/10.1016/j.jallcom.2021.162467.
24. Shpotyuk O., Kozyukhin S., Shpotyuk Ya. *et al*. Coordination disordering in near-stoichiometric arsenic sulfide glass. *J. Non-Cryst. Solids*. 2014. **402**. P. 236. https://doi.org/10.1016/j.jnoncrysol.2014.06.013.
25. Shpotyuk O., Kozyukhin S.A., Demchenko P.Yu. *et al.* Milling-driven nanonization of As_xS_{100-x} alloys from second glass-forming region: The case of lower-crystalline arsenicals ($56<x<66$). *J. Non-Cryst. Solids*. 2020. **549**. P. 120339. https://doi.org/10.1016/j.jnoncrysol.2020.120339.
26. V. Mitsa, R. Holomb, G. Lovas *et al*. Spectroscopic evidence of coexistence of clusters based on low (α) and high temperature (β) GeS_2 crystalline phases in glassy germanium disulfide matrix. *37th Int. Convention on Information and Communication Technology, Electronics and Microelectronics* MIPRO 2014/MEET. P. 13–16. https://doi.org/10.1109/MIPRO.2014.6859522.
27. Holomb R., Mitsa V., Johansson P. Localized states model of GeS_2 glasses based on electronic states of Ge_nSm clusters calculated by using TD-DFT method. *J. Optoelectron. Adv. Mater*. 2005. **7**. P. 1881–1888.
28. Shanelova J., Malek J., Alcala M., Criado J. Kinetics of crystal growth of germanium disulfide in $Ge_{42}S_{58}$ chalcogenide glass. *J. Non-Cryst. Solids*. 2005. **351**. P. 557–567. https://doi.org/10.1016/j.jnoncrysol.2005.01.042.
29. Armand P., Ibanez A., Philippot E. *et al*. Local and medium order in germanium chalcogenide glasses. *J. Non-Cryst. Solids.* 1992. **150**. P. 371–375. https://doi.org/10.1016/0022-3093(92)90155-D.
30. Micoulaut M., Phillips J.C. Rings and rigidity transitions in network glasses. *Phys. Rev. B*. 2003. **67**. P. 104204. https://doi.org/10.1103/PhysRevB.67.104204.
31. Stronski A.V., Kavetskyy T.S., Revutska L.O. *et al*. The boson peak and the first sharp diffraction peak in $(As_2S_3)_x(GeS_2)_{1-x}$ glasses. *SPQEO*. 2021. **24**. P. 312–318. https://doi.org/10.15407/spqeo24.03.312.
32. Gamulin O., Ivanda M., Mitsa V. *et al*. Monitoring structural phase transition of $(Ge_2S_3)_x(As_2S_3)_{1-x}$ chalcogenide glass with Raman spectroscopy. *J. Mol. Struct*. 2011. **993**. P. 264–268. https://doi.org/10.1016/j.molstruc.2011.01.059.

Author and CV

Volodymyr Mitsa, DSc, Professor at the Uzhhorod National University. He has authored 5 monographs, 10 textbooks, a book chapter (Springer), more than 400 scientific publications, and holds 9 USSR Invention Certificates. He has supervised 4 PhD and 1 Dr. Habil. (DSc) theses. Professor Mitsa is a member of the Ukrainian and American Physical Societies. His research focuses on the investigation of the structure and physical properties of chalcogenide glasses using spectroscopic methods.
https://orcid.org/0000-0001-8582-4698

Порівняння залежностей модулів пружності та густини від середнього координаційного числа для стехіометричних і нестехіометричних розрізів потрійних стекол Ge–As–S

В. М. Міца

Анотація. Досліджено бінарні As(Ge)–S та потрійні Ge–As–S стекла вздовж стехіометричних (квазібінарних) розрізів $As_{0.40}S_{0.60}$–$Ge_{0.33}S_{0.67}$ та нестехіометричних розрізів $As_{0.35}S_{0.65}$–$Ge_{0.35}S_{0.65}$, $As_{0.40}S_{0.60}$–$Ge_{0.40}S_{0.60}$, Ge–$As_{0.40}S_{0.60}$ з метою з'ясування ролі середнього координаційного числа (складу скла) у формуванні фізичних властивостей скла, зокрема модулів пружності та густини. Отримано нові дані про поведінку фізичних параметрів поблизу відомих «магічних» значень середнього координаційного числа, що має практичне значення для топологічної наноінженерії та розробки нових складів скла. Проведено порівняльний аналіз характеристик пружності та густини для розрізів, збагачених сіркою та германієм, відносно квазібінарного розрізу $As_{0.40}S_{0.60}$–$Ge_{0.33}S_{0.67}$. Структуру стекол розглянуто в межах концепції гетерогенного впорядкування при нанокластеризації під час гартування розплаву. Для встановлення кореляцій між властивостями та структурними характеристиками стекол (топологія, стехіометрія, розмірність) проаналізовано структуру кристалічних сполук різних типів, притаманних бінарним системам As(Ge)–S.
Ключові слова: бінарні As(Ge)–S стекла, потрійні Ge–As–S стекла, модуль пружності, густина, середнє координаційне число, структура стекол.